

RSC Advances



This is an *Accepted Manuscript*, which has been through the Royal Society of Chemistry peer review process and has been accepted for publication.

Accepted Manuscripts are published online shortly after acceptance, before technical editing, formatting and proof reading. Using this free service, authors can make their results available to the community, in citable form, before we publish the edited article. This *Accepted Manuscript* will be replaced by the edited, formatted and paginated article as soon as this is available.

You can find more information about *Accepted Manuscripts* in the [Information for Authors](#).

Please note that technical editing may introduce minor changes to the text and/or graphics, which may alter content. The journal's standard [Terms & Conditions](#) and the [Ethical guidelines](#) still apply. In no event shall the Royal Society of Chemistry be held responsible for any errors or omissions in this *Accepted Manuscript* or any consequences arising from the use of any information it contains.

Red Up-conversion Emission in α -KYb₃F₁₀:Er³⁺ Films Made by Electrodeposition

Received 00th January 20xx,
Accepted 00th January 20xx

DOI: 10.1039/x0xx00000x

www.rsc.org/

Xiaowen Wu, Linlin Tian, Qinyan Lu and Run Liu*

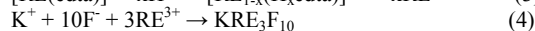
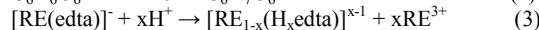
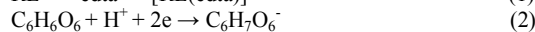
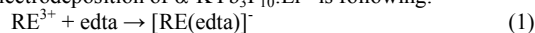
Er³⁺ ions doped α -KYb₃F₁₀ thin films were obtained from an aqueous solution through electrodeposition near room temperature. The annealed films show almost single band red emission excited by a 980 nm laser and two photons upconversion mechanism is involved.

Recently, there are considerable interests for lanthanide-doped up conversion (UC) phosphors owing to their applications in color 3D displays, solid-state lasers, bioimaging, and photovoltaics.¹⁻¹⁰ The UC phosphors normally exhibit multipeak emissions since lanthanide ions generally have more than one excited state.¹¹ To improve the chromatic purity of optical devices and reduce the absorption of tissue, a red-emitting up conversion phosphor with high color purity is vitally need. Thus, preparation of up conversion phosphors with single red emission is of technological importance and challenge.

For proceeding efficient up conversion, Yb³⁺ ions are doped in crystals as sensitizers due to the large absorption cross section of Yb³⁺ ions matched to 980 nm laser excitation sources and the efficient energy transition from Yb³⁺ to Er³⁺, Tm³⁺ and Ho³⁺ activators.¹ An increased amount of Yb³⁺ content would be likely to enhance the luminescence efficiency and also red-to-green emission ratio in Yb/Er co-doped fluoride crystals.¹²⁻¹³ Therefore, it is worth to explore the up conversion properties of Er³⁺ ions doped Yb-base fluorides. Moreover, for the device applications, a film of the UC based phosphors is requisite, and preferably made through a low-cost processing. Electrochemical deposition is a well-known solution process to prepare a functional film in an aqueous or non-aqueous solution.¹⁴⁻²⁰ This method has advantages of low temperature and low-cost in controlling the composition and structure of the deposited films.

In this work, we showed that Er³⁺ ions doped α -KYb₃F₁₀ thin films can be obtained by a facile anode electrodeposition process from aqueous solutions near room temperature. The annealed α -KYb₃F₁₀:Er³⁺ thin films exhibited almost single band strong red emissions upon excited with a 980 nm laser. Our results indicate that α -KYb₃F₁₀:Er³⁺ thin films may be used in new optical display devices and bioimaging.

The Er³⁺ doped α -KYb₃F₁₀:Er³⁺ films were electrodeposited on ITO electrode in an aqueous solution containing lanthanide ions-EDTA complexes and ascorbic acid. Under applied anode potentials (Experimental details were provided in supplemental materials), ascorbic acids are oxidized to generate H⁺ ions on the surface of ITO electrode.^{20,22} The released H⁺ ions will reduce the pH on the surface of the ITO electrode where the lanthanide ions can be set free from lanthanide ions-EDTA complex and then react with K⁺ and F⁻ ions to form KYb₃F₁₀:Er³⁺ deposits. The possible mechanism for anodic electrodeposition of α -KYb₃F₁₀:Er³⁺ is following:



where, RE³⁺ represents Yb³⁺ and Er³⁺ ions.

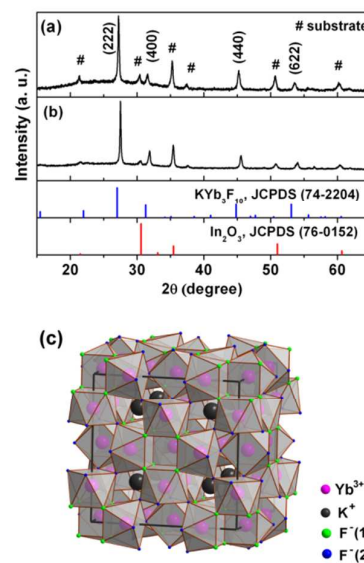


Fig.1. XRD patterns of the films electrodeposited at 0.8 V vs Ag/AgCl and 60 °C in 0.01 M Re-EDTA complexes, 0.1 M KF and 0.1 M ascorbic acid aqueous solution: (a) as electrodeposited α -KYb₃F₁₀:Er³⁺ (2 mol %) films; (b) electrodeposited α -KYb₃F₁₀:Er³⁺ (2 mol %) films annealed in air at 300 °C for two hours; (c) Crystal structure of α -KYb₃F₁₀.

Department of Chemistry, Zhejiang University, Hangzhou, 310027, china.
E-mail: runliu@zju.edu.cn

Electronic Supplementary Information (ESI) available: Details of experimental procedure. See DOI: 10.1039/x0xx00000x

Fig. 1a shows X-ray diffraction results of the as electrodeposited film containing 2 mol % Er^{3+} ions and the same film annealed at 300 °C in air for two hours. Both XRD patterns can be indexed as reported cubic $\alpha\text{-KYb}_3\text{F}_{10}$ (JCPDS: 74-2204) structure.²¹ Besides XRD pattern of the ITO substrate, there is no other impure phase. The lattice parameter of the electrodeposited $\alpha\text{-KYb}_3\text{F}_{10}$ is $a = 11.338 \text{ \AA}$, a little less than the reported value ($a = 11.431 \text{ \AA}$).²¹ The sharp and strong peaks indicate that as electrodeposited and annealed $\alpha\text{-KYb}_3\text{F}_{10}:\text{Er}^{3+}$ thin films are well crystallized. The films show a little [111] preferred orientation. Fig. 1b shows the crystal structure of $\alpha\text{-KYb}_3\text{F}_{10}$. The crystal structure of $\alpha\text{-KYb}_3\text{F}_{10}$ is isotopic with $\gamma\text{-KYb}_3\text{F}_{10}$, a cubic $2 \times 2 \times 2$ superstructure of fluorite that consists of two ionic groups $[\text{KYb}_3\text{F}_8]^{2+}$ and $[\text{KYb}_3\text{F}_{12}]^{2-}$ alternating along the three crystallographic directions.²¹ The coordination of the Yb^{3+} ions in the $\alpha\text{-KYb}_3\text{F}_{10}$ structure is square antiprismatic with C_{4v} symmetry.

Fig. 2a and 2b show typical scanning electron microscopy (SEM) images of the electrodeposited and annealed $\alpha\text{-KYb}_3\text{F}_{10}:\text{Er}^{3+}$ (2 mol %) films, respectively. Both films are composed of spherical structures with size of around 400 nm in diameter and the annealing process does not change the morphology too much. Fig. 2c shows that the thickness of the annealed film obtained by cross-section SEM image is about 550 nm. Fig. 2d shows that there are K, F, Yb and Er elements existed in the annealed films in the Energy Dispersive X-ray Spectrum (EDX). Based on the result of EDX, the content of the Er^{3+} ions in the films is consistent with the amount of Er^{3+} ions in the solution. Fig. 2e and 2f further show that Yb^{3+} and Er^{3+} ions are homogeneously distributed in $\text{KYb}_3\text{F}_{10}$ films.

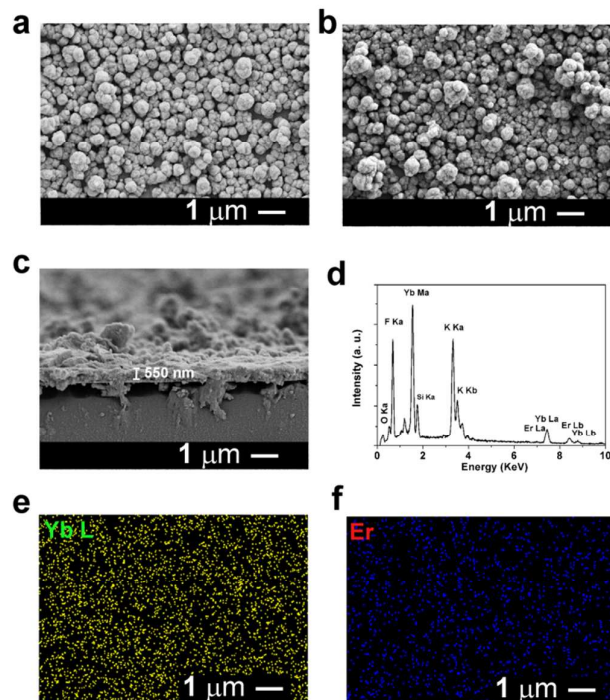


Fig. 2 SEM images of films electrodeposited at 0.8V vs Ag/AgCl and 60 °C from 0.01M Re-EDTA complexes, 0.1M KF and 0.1M ascorbic acid aqueous solution: a) as electrodeposited $\alpha\text{-KYb}_3\text{F}_{10}:\text{Er}^{3+}$ (2 mol %) films b) electrodeposited $\alpha\text{-KYb}_3\text{F}_{10}:\text{Er}^{3+}$ (2 mol %) annealed at 300°C for 2 h. c) the cross-section image of the annealed film. d) EDX spectrum of annealed electrodeposited $\alpha\text{-KYb}_3\text{F}_{10}:\text{Er}^{3+}$ (2 mol %) films. e) and f) EDX mapping images of the annealed electrodeposited $\alpha\text{-KYb}_3\text{F}_{10}:\text{Er}^{3+}$ (2 mol %) films.

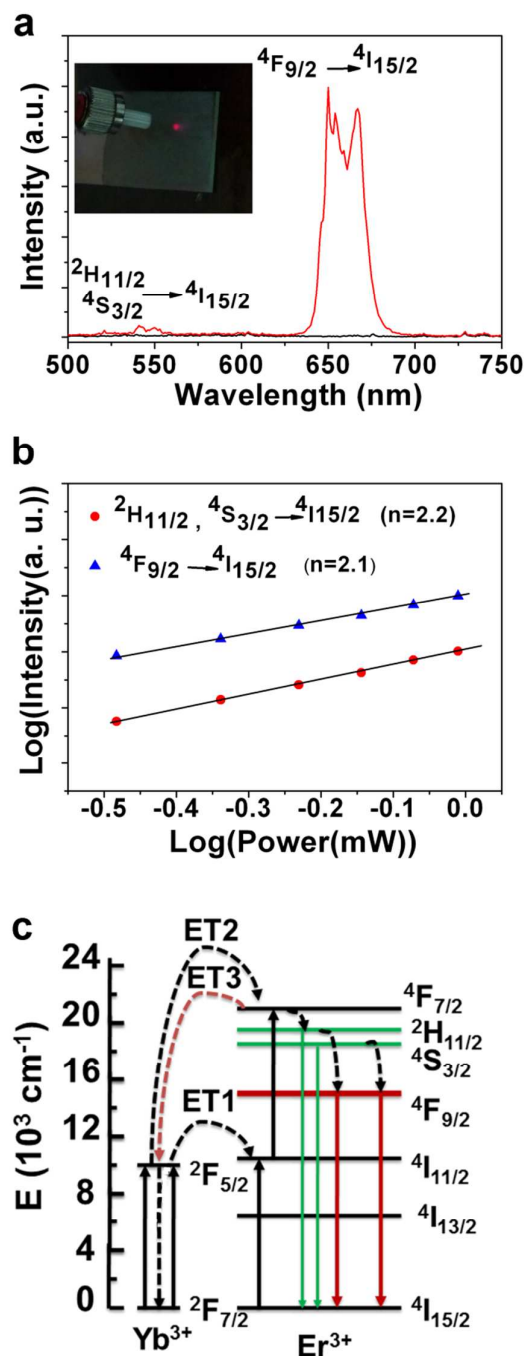


Fig. 3 a) UC emissions of as electrodeposited (black line) and annealed electrodeposited (red line) $\alpha\text{-KYb}_3\text{F}_{10}$ film doped with 2 mol % Er^{3+} ions. Inset image is the film excited with a 0.5 W 980 nm laser. (b) Power dependence of the UC emissions excited at 980 nm. (c) The energy level diagrams of Er^{3+} and Yb^{3+} ions and up conversion mechanism excited at 980 nm.

The up-conversion emissions of as electrodeposited and annealed $\alpha\text{-KYb}_3\text{F}_{10}:\text{Er}^{3+}$ (2 mol %) films under excitation by a 980 nm laser were investigated. The as electrodeposited $\alpha\text{-KYb}_3\text{F}_{10}:\text{Er}^{3+}$ films show little emissions (shown in Fig. 3a using black line). Similar result was also observed in our previous works.²² Two possible paths decrease the emission

intensity, one is the change of crystal structure of the host and the other one is the surface effects. The XRD patterns and width of (111) peak of electrodeposited and annealed electrodeposited films are compared and there are little differences (Fig.S1). This indicates that the annealed process has little effect on the crystal structure and grain size of the electrodeposited films due to low annealed temperature (350 °C). Thus the change crystal structure of the annealed films is excluded on affecting the emission intensity. The surface effects on emission intensity are attributed to the presence of high vibrational energy ligands (e.g., -CH, -OH groups) or surface defects (e.g., vacancy, lanthanide segregation).²³⁻²⁵ The -OH groups are known to be efficient quenchers in Ln³⁺-doped phosphate glass and NaYF₄:Yb,Er nanocrystals.^{24,26} The Fourier transform infrared (FTIR) spectra of the electrodeposited and annealed electrodeposited KYb₃F₁₀ are compared (Fig.S2). The absorption of -OH group in annealed films decreases dramatically and -CH groups change little. Therefore, the emission might be annihilated by adsorbed water in the as electrodeposited α -KYb₃F₁₀:Er³⁺ films obtained from aqueous solution.

For annealed films, Fig.3a shows that there are a weak green emission at 542 and 549 nm and a strong red emission peak at 654 nm. The ratio of red/green is about 22.5 for the annealed α -KYb₃F₁₀:Er³⁺ (2 mol %) film. Inset image in Fig.3a shows that the annealed film exhibits intense red emission upon excited with a 0.5 W 980 nm laser. The green emission bands at 542 and 549 nm accounts for the ²H_{11/2}, ⁴S_{3/2} → ⁴I_{15/2} transition and the red luminescence centered at 654 nm is ascribed to the ⁴F_{9/2} → ⁴I_{15/2} transition of Er³⁺, respectively. The quantum efficiency of the film is measured by the method developed by Zhang and Zhao²⁷ and is about 0.036%, which is higher than our reported value in electrodeposited NaGdF₄:Yb³⁺/Er³⁺ film.²²

To investigate the up conversion mechanism of α -KYb₃F₁₀:Er³⁺, the intensities of the up conversion emissions were recorded as a function of the power of 980 nm laser. For an unsaturated up conversion process, the emission intensity (I) is proportional to power (n) of laser power (P):

$$I \propto P^n \quad (5)$$

where n represents the number of infrared photons absorbed per visible photo emitted.²⁸ Fig.3b shows a plot of log[I] versus log[P] and their slopes are used to determine the value of n. As can be seen in the inset, slopes of 2.2 and 2.1 are obtained. This indicates that ⁴F_{9/2} → ⁴I_{15/2} and ⁴S_{3/2} → ⁴I_{15/2} transition come from two photons up conversion processes.

Therefore, the energy level diagrams of Er³⁺ and Yb³⁺ ions as well as the up conversion mechanism are presented in Fig.3c. Firstly, Yb³⁺ ion is excited to ²F_{2/5} state by absorbing a near-infrared photon, and then the state ⁴I_{11/2} of Er³⁺ is populated by energy transfer (ET1) occurred from Yb³⁺ ion to Er³⁺ ion. In the meantime, Er³⁺ ion itself can also absorb a 980 nm photon directly from the laser. Another energy transfer (ET2) between Yb³⁺ and Er³⁺ can populate the ⁴F_{7/2} level of the Er³⁺ ion. Then Er³⁺ ion relax non-radiatively to the ²H_{11/2} and ⁴S_{3/2} levels. When ²H_{11/2} → ⁴I_{15/2} and ⁴S_{3/2} → ⁴I_{15/2} transitions of Er³⁺ ions occur, green light can be observed. As for red light emission, it comes from ⁴F_{9/2} → ⁴I_{15/2} transition. There are two pathways for the population of ⁴F_{9/2} level. One is the relaxation of ²F_{7/2} and the other is excitation from ⁴I_{13/2} by the energy transfer of Yb³⁺ or absorption of a 980 nm photon.²⁹ It was reported that an ET3 process: ⁴F_{7/2}(Er) + ²F_{7/2}(Yb) → ⁴I_{11/2}(Er) + ²F_{5/2}(Yb),³⁰ can depopulate the ⁴F_{7/2} excited level and reduce the intense of green emission. Therefore, the red emission is dominated in the electrodeposited α -KYb₃F₁₀:Er³⁺ films.

In summary, we have demonstrated that α -KYb₃F₁₀:Er³⁺ thin films shown nearly single red emissions excited by a 980nm

laser can be obtained from an aqueous solution by a facile electrodeposition method near room temperature. It is expected that the α -KYb₃F₁₀:Er³⁺ thin films on transparent ITO substrate will be suitable for applications in optical display devices and bioimaging.

Acknowledgements

This work was financially supported by National Natural Science Foundation of China (21373183), the National Basic Research Program of China (Grant No. 2011CB936003), and Zhejiang Provincial Natural Science Foundation of China (LY12B07001).

Notes and references

1. F. Auzel, *Chem. Rev.*, 2004, **104**, 139.
2. E. Downing, L.Hesslink, J.Ralston, R. Macfarlane, *Science*, 1996, **273**, 1185.
3. T. Sandrock, H. Scheife, E. Heumann, G. Huber, *Opt. Lett.*, 1997, **22**, 808.
4. B.E. Cohen, *Nature*, 2010, **467**, 407.
5. G. Wang, Q. Peng, Y. Li, *Acc. Chem. Res.*, 2011, **44**, 322.
6. A. Shalav, B. S. Richards, T. Trupke, K. W. Krämer, H. U. Güdel, *Appl. Phys. Lett.*, 2005, **86**, 013505-1.
7. M. Haase, H. Schäfer, *Angew. Chem. Int. Ed.*, 2011, **50**, 5808.
8. B. M. van der Ende, L. Aarts, A. Meijerink, *Phys. Chem. Chem. Phys.*, 2009, **11**, 11081.
9. N. Menyuk, K. Dwight, J. W. Pierce, *Appl. Phys. Lett.*, 1972, **21**, 159.
10. R. T. Wegh, H. Donker, K. D. Oskam, A. Meijerink, *Science*, 1999, **283**, 663.
11. J. F. Suyver, J. Grimm, K. W. Krämer, H. U. Güdel, *J. Lumin.*, 2005, **114**, 53.
12. F. Wang, X. Liu, *J. Am. Chem. Soc.* 2008, **130**, 5642
13. D. Chen, L. Lei, R. Zhang, A. Yang, J. Xu, Y. Wang, *Chem. Commun.*, 2012, **48**, 10630.
14. J. A. Switzer, G. Hodes, *MRS Bulletin*, 2010, **35**, 743.
15. R. M. Penner, *J. Phys. Chem. C*, 2014, **118**, 17179.
16. M. J. Siegfried, K-S Choi, *Angew. Chem. Int. Ed.*, 2005, **44**, 3218.
17. T. Yoshida, H. Minoura, *Adv. Mater.*, 2000, **16**, 1219.
18. D. Lincot, *Thin Solid Films*, 2005, **487**, 40.
19. M. Dinamani, P. V. Kamath, R. Seshadri, *Chem. Mater.*, 2001, **13**, 3981
20. S. J. Limmer, E. A. Kulp, J. A. Switzer, *Langmuir*, 2006, **22**, 10535.
21. M. Labeau, S. Aleonard, A. Vedrine, R. Boutonnet, J. C. Cousseins, *Mat. Res., Bull.*, 1974, **9**, 615.
22. L. Tian, P. Wang, H. Wang, R. Liu, *RSC Adv.*, 2014, **4**, 19896.
23. M. C. Tan, G. A. Kumar, R. E. Riman, M. G. Brik, E. Brown, U. Hommerich, *J. Appl. Phys.*, 2009, **106**, 063118.
24. Y. Yan, A. J. Faber, H. de Waal, *J. Non-Cryst. Solids*, 1995, **181**, 283.
25. F. Wang, J. Wang, X. Liu, *Angew. Chem. Int. Ed.*, 2010, **49**, 7456.
26. D. Yuan, M. C. Tan, R. E. Riman, G. M. Chow, *J. Phys. Chem. C*, 2013, **117**, 13297.
27. X. M. Li, D. K. Shen, J. P. Yang, C. Yao, R. C. Che, F. Zhang, D. Y. Zhao, *Chem. Mater.*, 2013, **25**, 106.
28. M. Pollnau, D. R. Gamelin, S. R. Luthi, H. U. Güdel, M. P. Hehlen, *Phys. Rev. B*, 2000, **61**, 3337.
29. J. Wang, R. R. Deng, M. A. MacDonald, B. L. Chen, J. K. Yuan, F. Wang, D. Z. Chi, T. S. A. Hor, P. Zhang, G. K. Liu, Y. Han, X. Liu, *Nature Mater.*, 2014, **13**, 157.
30. H. Guo, N. Dong, M. Yin, W. Zhang, L. Lou, S. Xia, *J. Phys. Chem. B* 2004, **108**, 19205.